

Interaction of Estuarine Morphology and adjacent Coastal Water Tidal Dynamics (ALADYN-C)

Krischan Hubert¹, Andreas Wurpts² and Cordula Berkenbrink²

¹ Nds. Landesbetrieb für Wasserversorgung, Küsten- und Naturschutz,
krischan.hubert@nlwkn.niedersachsen.de

² Nds. Landesbetrieb für Wasserversorgung, Küsten- und Naturschutz

Summary

Long term tidal dynamic changes comprise a share of multiple possible influencing processes. In the shallow Wadden Sea in the south eastern German Bight, morphological changes – both natural and those manmade – are key contributors, as coastal relief and tidal wave are shaping and interacting with each other. Several publications have analysed, how bathymetrical changes in the estuarine zone due to river construction measures influence the tidal regime inside the investigated entity. This study aims at identifying, how far those tidal dynamic changes will have an impact on adjacent coastal waters and give an estimate how they are reflected in the data of surrounding tide gauges. The investigation is based on comparisons of tidal characteristics for different morphological conditions of selected regions along the German coastline by means of numerical modelling. A cross-scale model domain was set up to simulate the hydrodynamics of the entire Greater North Sea with a special focus on the highly resolved German tidal waters. Digitized historical conditions for the Ems and Weser estuary prior to major human activities along the rivers were used to reproduce the tidal regime of the corresponding time period within the large-scale environment of the overall domain. Morphological changes that account for single measures, such as the land subsidence due to gas extraction, were analysed isolated from other changes. The differences of the simulation results are compared to values from control runs with the present bathymetrical state. This illustrates the region of influence, in which tides are effected from locally limited bathymetrical changes.

Keywords

tidal dynamics, sea level rise, long-term trend, estuary, Ems, Weser, North Sea, historic bathymetry, coastal morphology, cross-scale modelling, land subsidence due to gas extraction, ALADYN, SCHISM

Zusammenfassung

Langzeitänderungen der Tidedynamik setzen sich aus einer Vielzahl von möglichen ursächlichen Prozessen zusammen. Im flachen Wattenmeer haben morphologische Veränderungen – sowohl natürlicher als auch anthropogen geprägter Art – einen entscheidenden Einfluss, da sich Tidewelle und Küstenrelief gegenseitig stark beeinflussen und formen. Mehrere wissenschaftliche Arbeiten haben bereits untersucht, inwiefern Änderungen der Bathymetrie von Ästuaren im Zuge von Flussausbauten das Tideregime innerhalb des

betrachteten Gebiets beeinflussen. Dieser Beitrag geht der Frage nach, wie weit sich diese Änderungen der Tidedynamik auch in außerhalb liegenden Gebieten feststellen lassen. Die Untersuchungen basieren auf Vergleichen von Tidekennwerten, die mittels numerischer Modellierung für verschiedene morphologische Zustände ausgewählter Abschnitte der deutschen Nordseeküste nachgebildet wurden. Für diesen Zweck wurde ein skalenübergreifendes Strömungsmodell erstellt, welches die Hydrodynamik des gesamten Nordseegebietes simuliert. Im Fokus der Untersuchungen stehen dabei die im Modellgebiet hochaufgelösten deutschen Tidegewässer. Digitalisierte Bathymetrie-Datensätze von historischen Ausbauzuständen der Ems und Weser, die bis vor die maßgebenden menschlichen Eingriffe in die Flussläufe zurückreichen, wurden verwendet, um die lokalen Gezeiten der entsprechenden Zeiträume innerhalb des gesamtübergreifenden Modellgebietes abbilden zu können. Veränderungen, die auf Einzelmaßnahmen zurückzuführen sind, wie Bodensenkungen infolge von Gasentnahme, werden isoliert von anderen Einflussfaktoren analysiert. Die Differenzen der Simulationsergebnisse aus dem Vergleich mit Werten aktueller Ausbauzustände stellen den Einflussbereich dar, in welchem lokal begrenzte Änderungen der Bathymetrie das Tideregime beeinflussen.

Schlagwörter

Tidedynamik, Meeresspiegelanstieg, Trend, Ästuar, Ems, Weser, Nordsee, historische Bathymetrie, Küstenmorphologie, skalenübergreifendes HN-Modell, Landsenkung infolge Gasentnahme, ALADYN, SCHISM

1 Introduction

The motivation for the joint research project ALADYN was to gain a better understanding of the composition of observed tidal range changes within the German Bight. Therefore, the three separate parts of the project would each aim on identifying and analysing different potential factors that may have contributed to the observed trends. One task within ALADYN was to analyse tidal regime changes induced by local bathymetrical changes. The goal of this project part was to analyse how far local hydrodynamic changes would spread into adjacent coastal regions. The focus is on the region around the estuaries Ems and Weser, both entering the North Sea at the Lower Saxonian coastline.

The hydrodynamics of the German Bight, its coastal morphology and a vast number of natural processes as well as human activities are greatly dominated by the influence of the tides. Along the coastline, there are numerous tide gauges, some of which are already in operation since up to over 150 years. Figure 1 shows yearly mean tidal high (MHW) and tidal low water (MLW) levels for selected gauge stations throughout the German Bight since begin of their operation.

Trend analysis of long-term tide records indicate a general increase of both MHW and MLW with rates of several centimetres up to a few decimetres within one century. Whereas the trends of the high waters are rather similar throughout the different gauge stations, trends in low waters are slightly diverse, as the low waters might react stronger on local morphological variations due to greater influence of bottom friction. For example, the low waters near the estuaries – i. e. Bremerhaven and Emden - seem to decrease due to the constant deepening of the neighbouring navigational channels. But there is one trend that is valid for all gauge stations: The MLW is always either falling or rising less strong than the corresponding MHW. Thus, the rates of mean tidal range (MTR) increase are all positive (see Table 1).

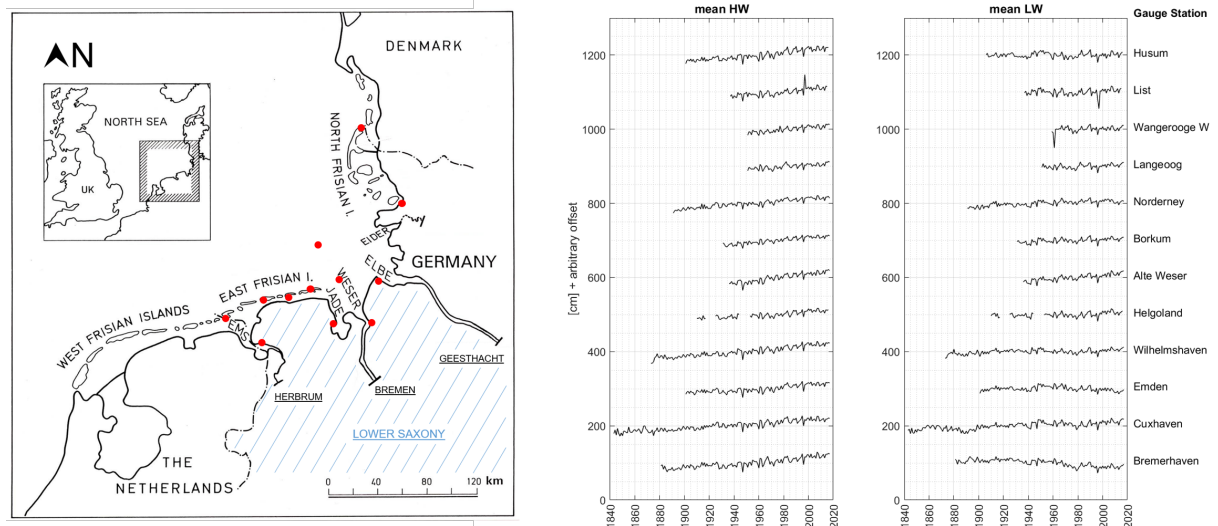


Figure 1: Left panel: Overview. Middle and right panel: Yearly mean tidal high and low waters [cm] with arbitrary offset at different gauge stations throughout the German Bight. The positions are indicated in the left panel. Data provided by German Federal Waterways and Shipping Administration (WSV).

The observed trends are composed from a variety of different processes that all contribute with different magnitudes and signs and that may interact linearly and non-linearly with each other. In addition to global factors like sea level rise, vertical land movement, variations in wind climate or astronomical constellations, changes of the tidal regime can also mirror local effects (Haigh, 2020). Morphology is a key factor on such local scales, especially in shallow coastal zones. Here the tidal regime is dominated by the bathymetry and correspondingly susceptible to morphological changes (Niemeyer and Kaiser 1999). The Wadden Sea represents an inherently morphodynamical system, which is subject to continuous rearrangement. Contributors are naturally imposed shifts and transformations of the tidal channels, flats, basins and barrier islands as well as anthropogenically induced changes due to navigational purposes or demands of coastal protection (Elsebach et al. 2007, Herrling and Niemeyer 2008).

In both Weser and Ems estuary, the major human interventions and consecutive morphological reactions started more than 130 years ago. After smaller previous measures the so-called Franzius corrections started in 1887 and were the beginning of a substantial rearrangement of the Outer and Lower Weser riverbeds, in order to obtain the access of the port of Bremen to the open sea. The corrections comprised a transition from a fairly shallow, curvy and branched riverbed to a deeper, comparatively narrow and single-branched channel (Elsebach et al. 2007, Franzius 1888, Niemeyer, 2000). Several consecutive adaptations of the river for increasing navigational demands followed up to present times (BUND, Portal Tideweser).

Considering the tidal range, the modifications engendered a drastic amplification of the tidal wave amplitude along the estuaries. Figure 2 displays the change of tidal range over time for lower Weser and Ems rivers. Before the Franzius corrections, the tidal wave was almost completely damped on its way through the estuary while today it is fully reflected and also steepened with strongly amplified range. At the head of the estuary, the present tidal range exceeds the one at the mouth, whereas it used to be close to zero before the corrections.

The evolution of the Ems estuary's morphology follows a similar pattern (Herrling and Niemeyer 2007b). Here, modifications also started in the second half of the 19th century, but continuous tide gauge records do not date back as long as for the Weser.

Table 1: Linear trends [mm/a] of yearly mean tidal high water, low water and tidal range values for the time of recording at different gauge stations throughout the German Bight. The positions are indicated in Figure 1. Data provided by WSV.

Tide gauge	Period	Linear trends [mm/a]		
		MHW	MLW	MTR
Husum	1901 – 2016	3.28	0.11	3.17
List	1937 – 2015	3.36	0.47	2.89
Wangerooge West	1951 – 2017	3.34	1.60	1.74
Langeoog	1951 – 2017	2.38	1.10	1.28
Norderney Hafen/Riffgat	1891 – 2017	2.80	1.33	1.47
Borkum Südstrand /Fischerbalje	1931 – 2017	3.09	1.18	1.91
Leuchtturm Roter Sand/Alte Weser	1936 – 2017	4.49	2.84	1.65
Helgoland Binnenhafen	1910 – 2016	2.16	0.72	1.44
Wilhelmshaven Alter Vorhafen	1873 – 2017	2.93	0.65	2.28
Emden Neue Seeschleuse	1901 – 2017	2.33	-0.29	2.62
Cuxhaven Steubenhöft	1843 – 2017	2.25	1.31	0.94
Bremerhaven Doppelschleuse/Alter Leuchtturm	1881 – 2017	2.74	-1.68	4.42

The anthropogenic interventions caused significant changes of the tidal regime within the estuaries of Ems and Weser itself. Those effects have already been thoroughly analysed with hydrodynamic modelling approaches (Elsebach et al. 2007, Herrling and Niemeyer 2008, Herrling et al. 2014).

This project is expanding the existing scope of the investigations. It is not only dealing with the tidal regime changes within the estuaries, but also whether how strong and how far these inner-estuarine changes also affect the adjacent coastal waters and tidal gauges located there. We examine possible interactions of the estuaries with the coastal zone and analyse, how far the hydrodynamic changes spread outside of the region of the corresponding morphological changes. This objective is addressed using numerical simulations of the large-scale tidal dynamics with comparisons between present and historical morphological conditions. The method allows to analyse single measurements or regions isolated from surrounding morphological changes. This way, shares of tidal characteristic changes can be assigned to certain events including the nonlinear behaviour of the hydrodynamics.

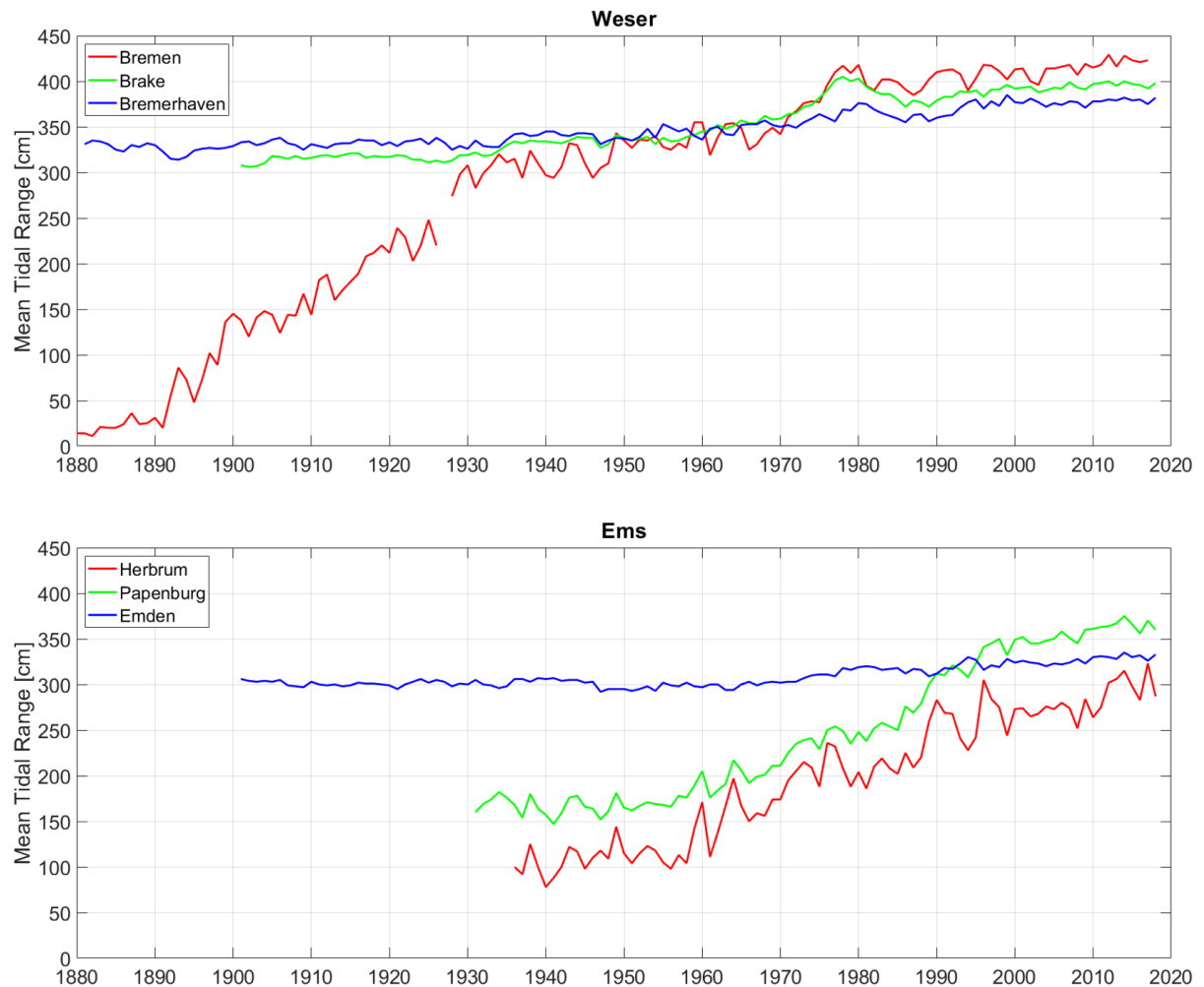


Figure 2: Yearly mean tidal range values [cm] along the Weser (upper panel) and Ems (lower panel) estuaries from 1880–2018. Red lines indicate a position near the head of the estuary, blue lines near the mouth and green lines approximately half way in between. Data provided by WSV. (Elsebach et al. 2007 and Niemeyer 2000 (unpublished)).

2 Methodology

For the purpose of this study a numerical model domain was set up, that not only covers the investigation area but is well extended above the Greater North Sea into parts of the North East Atlantic. This approach offers several advantages over models with smaller extend or nested cascades of models:

- It bypasses model cascades, as the tidal oscillations at the seaward open boundaries can be forced directly through tidal constituent phases and amplitudes in the open ocean. Due to the great distance between open boundary and investigation area, the velocity boundary condition can be omitted.
- The propagation of the tidal wave is physically consistent throughout the entire model domain. There is a bi-directional interaction between the coastal zone and the open sea, which would be missing in a one-way nested application. Influences from model boundary forcing are avoided.

- The investigation area is not limited pre-hand to an inner domain or specific region. This is an important factor, as the spatial distribution is part of the analysis and is considered as unknown initially.

The procedure of the evaluation of morphologically induced tidal regime changes happens as follows: For each analysis we perform two simulations on the same numerical grid, which is beforehand optimized for two morphological states. The first simulation is the control run. It contains the present state bathymetry and is equal for all analysis. The bathymetry of the second simulation is replaced by a historical data set in the respective area of interest. All remaining parts of the model and all boundary conditions remain exactly the same. After calculating the differences of certain tidal characteristics between the two simulations, it is possible to derive spatial information on how far these differences exceed the manipulated area.

Analysis are carried out over a period of at least two spring-neap cycles. For the comparisons, synthesized mean tidal curves for elevation and u- and v-velocities are derived from all single tidal cycles for each computational node in the domain. This procedure ensures that the calculated differences comprise an average over the diurnal, fortnightly and monthly inequalities of the tide. It is not only an average of single parameters like peak and crest heights or maximum flood and ebb velocities. The synthesized tidal curve displays an averaged tidal curve over 12.4 hours with a temporal discretization of six minutes (see Section 3).

2.1 Model Setup

The simulations are carried out with the semi-implicit, finite element model suite SCHISM (Zhang et al. 2016, version 5.6.1) which is tailored to seamless cross-scale applications. The domain is – in the horizontal plane – discretized with an unstructured grid of triangular and quadrangular elements.

Figure 3 gives an overview of the model domain. The western seaward open boundary spans from the north-western tip of Spain across the Atlantic at $\sim 16^\circ$ west up to Iceland. The northern seaward open boundary spans from Iceland across the Norwegian Sea down to western Norway. The most easterly part of the model is the Kattegat. The model boundary towards the Baltic Sea follows the coast of the Danish major islands Funen and Zealand, connecting the Danish and Swedish mainland. The connecting belts to the Baltic Sea are not considered as open boundaries, as we consider the influence it has on the investigation area in the German Bight as insignificant, especially as it would have to encounter the net-direction of both the Norwegian and so-called “Silberrinnen” tidal wave (See- und Ozeanhandbücher 1958). In the German Bight, the different entities of the Wadden Sea – tidal inlets, tidal basins and barrier islands – are resolved. The model includes the estuaries of the Ems, Weser and Elbe rivers up to their tidal barriers in Herbrum, Bremen and Geesthacht respectively. Also parts of the tidal Eider River are included in the Model domain. Ems, Weser and Elbe River are supplied with discharge open boundaries. The discharge boundaries are located upstream of the tidal barriers which are represented by weir structures in the model (Ateljevich et al. 2014). Tributaries of Ems and Weser River as well as the Eider River are treated as sources.

The SCHISM model enables maximum flexibility for the horizontal discretization. Because the terms imposing the most stability constraints are handled numerically implicit

and advection of momentum is treated by means of an un-Trim-like Lagrange approach, a wide range of different mesh sizes is possible, as Courant numbers far beyond 1 are possible (Zhang et al. 2016). We highly resolve the investigation area around the estuaries and the Wadden Sea and have a very coarse resolution in the Greater North Sea and Atlantic parts of the model. This way, around 90 % of the ~ 675 thousand horizontal computational nodes and ~ 1.2 million elements are inside the investigation area, which in contrast only covers less than 1 % of the model domain (compare Table 2). Consequently, the large overall domain has little effect on the computational time.

Table 2: Numbers of grid nodes, area size and Element size range for different regions of the model domain. Values are only approximate.

Region	number of nodes	Share of nodes %	Area km^2	Share of Area %	Element size range m
Inner estuaries of Ems Weser Elbe	100000	14.8	1100	0.05	5* – 200
Wadden Sea	500000	74.1	15000	0.65	50 - 200
Remaining Greater North Sea	50000	7.4	700000	31.15	200 – 10000
Remaining Model domain	25000	3.7	1530000	68.15	3000 – 50000
Total	675000	100.0	2246100	100.00	5 - 50000

*direction of quad. elements perpendicular to flow direction

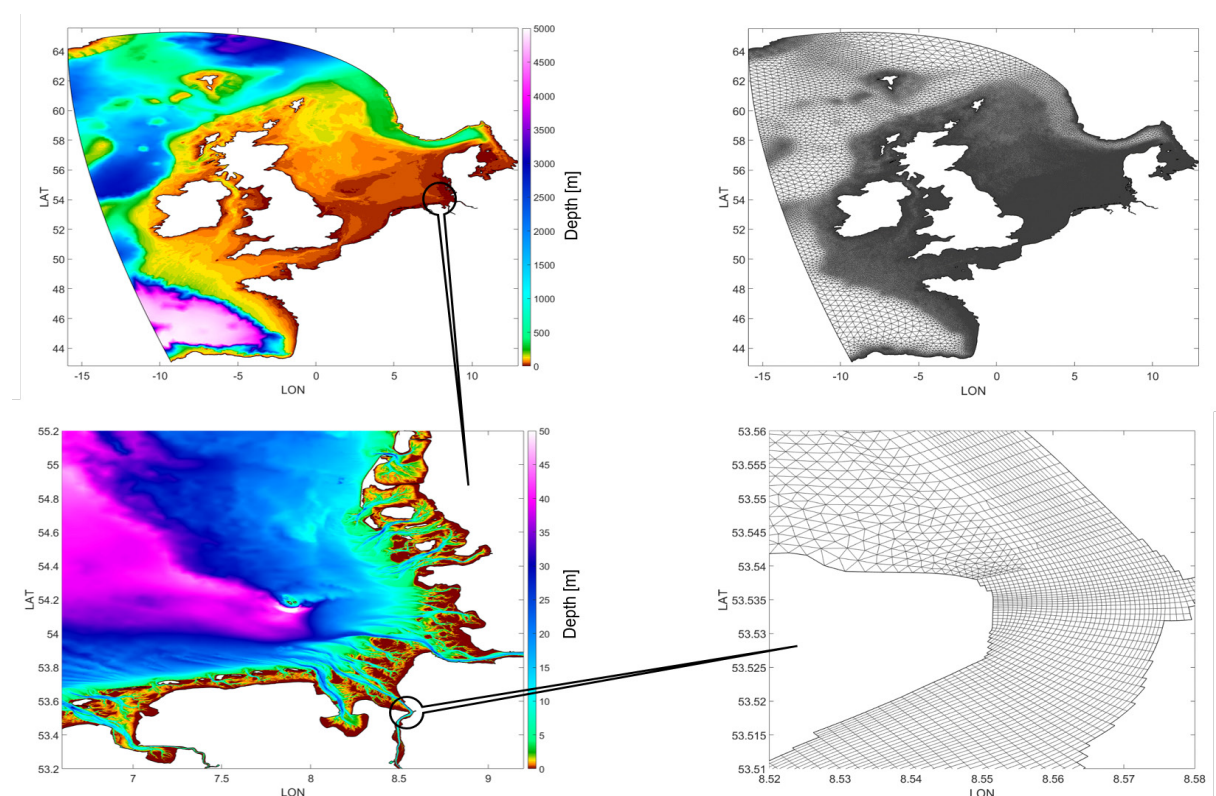


Figure 3: Overview of the model domain (Hubert et al. 2019). Top left panel shows the spatial extent, colors indicate the bathymetry. Bottom left panel shows the German Bight as an enlarged detail of the model. Top right panel shows the unstructured horizontal grid, which's local resolution is aligned with respect to the corresponding model depth. Bottom right panel shows an exemplary transition from triangular to quadrangular elements at the head of Lower Weser estuary.

The majority of elements are of triangular shape. Their sizes are determined by the surrounding depth (compare Figure 3). In the channels of Ems and Weser as well as in selected tidal channels, where there occurs distinct bidirectional flow, quadrangular elements are used to ensure a proper representation of the channels cross-sections and further reduce numerical diffusion and element numbers. As the Ems river gets comparatively narrow close to its tidal barrier, element sizes perpendicular to the flow direction go under 10 meters, in order to assure a minimum number of five to six active nodes in the cross-section during low water conditions. In the vertical discretization, localized sigma coordinates (LSC²) are used (Zhang et al. 2015).

Bathymetrical information for the model is compiled from several sources (compare Table 3). In the larger domain of the Greater North Sea and Atlantic we use open source data from EasyGSH-DB and EMODnet. Within the Lower Saxony Coastal Zone and estuaries, we use state owned high-resolution LiDAR and sounding data. Bathymetry for the tidal parts of the Eider River were provided by the Schleswig-Holstein Agency for Coastal protection, National park and Marine Conservation.

Table 3: Present and historic bathymetries used in the numerical model

Region	Period*	Source
Present		
Atlantic and parts of the North Sea	2016	EMODnet
German Bight and parts of the North Sea	2016	EasyGSH-DB
Parts of the tidal Eider River	2012	State of Schleswig Holstein
Ems estuary	2015	State of Lower Saxony
Jade Estuary	2012	State of Lower Saxony
Weser estuary	2012	State of Lower Saxony
Elbe estuary	2010	State of Lower Saxony
East Frisian islands	2013- 2016	State of Lower Saxony
Historic		
Entire Lower Saxony coastline	1650, 1750, 1860, 1960	Homeier et al. 2010
Ems	1937	Herrling and Niemeyer 2007a
Lower Weser	1887	Elsebach et al. 2007
Outer Weser	1870	Dev. within this project
East Frisian islands	1960	Dev. within this project

* data might not be limited to a single year but cover a larger time span

Considering the historical bathymetries, a number of data sets have been developed within former research work as well as within this research project. They have been developed by comprehensive digitization of historic navigational charts or other ancient documents. Figure 4 shows exemplarily the setup of the historic bathymetry of the outer Weser estuary.

Because bathymetrical information more than a hundred years ago was sparse – both in space and time – as well as much less accurate compared to today’s possibilities, there are a few limitations that need to be pointed out:

- The historical data sets, especially for larger areas, never represent a close instant of time. The preparation of navigational charts in 19th and early 20th century took several

measuring campaigns to complete and thus are compiled from data that was collected over a period of sometimes several years.

- For larger areas, there are sometimes not enough maps of the same period available to cover the whole area, or certain maps have to be omitted due to insufficient quality or other reasons. For example, the historical bathymetry for the Ems estuary is compiled from different maps covering several decades (Herrling and Niemeyer 2007a).
- As ancient maps were mainly created for navigational purposes, information outside the navigational channels, i.e. tidal flats, are provided only with little depth information. These gaps have to be filled with assumptions.
- The vertical reference system differs from today's vertical reference and thus depths need to be adjusted. In some cases, depth will be given with reference to local low water marks. Here, adjustment of the depths is a lot more difficult, as it has to be done with historical tide gauge data.

Also present bathymetrical data sets face some of these problems, especially when looking at the larger offshore domain of the North Sea, where on the one hand depth are still shallow, so that inaccuracies can have a notable impact on the simulated tide but on the other hand such inaccuracies are unavoidable with respect to the size of the area and the absence of GNSS kinematic reference.

Therefore it is very important to straighten out that the derived results in this study must always be looked at with respect to the range of uncertainties.

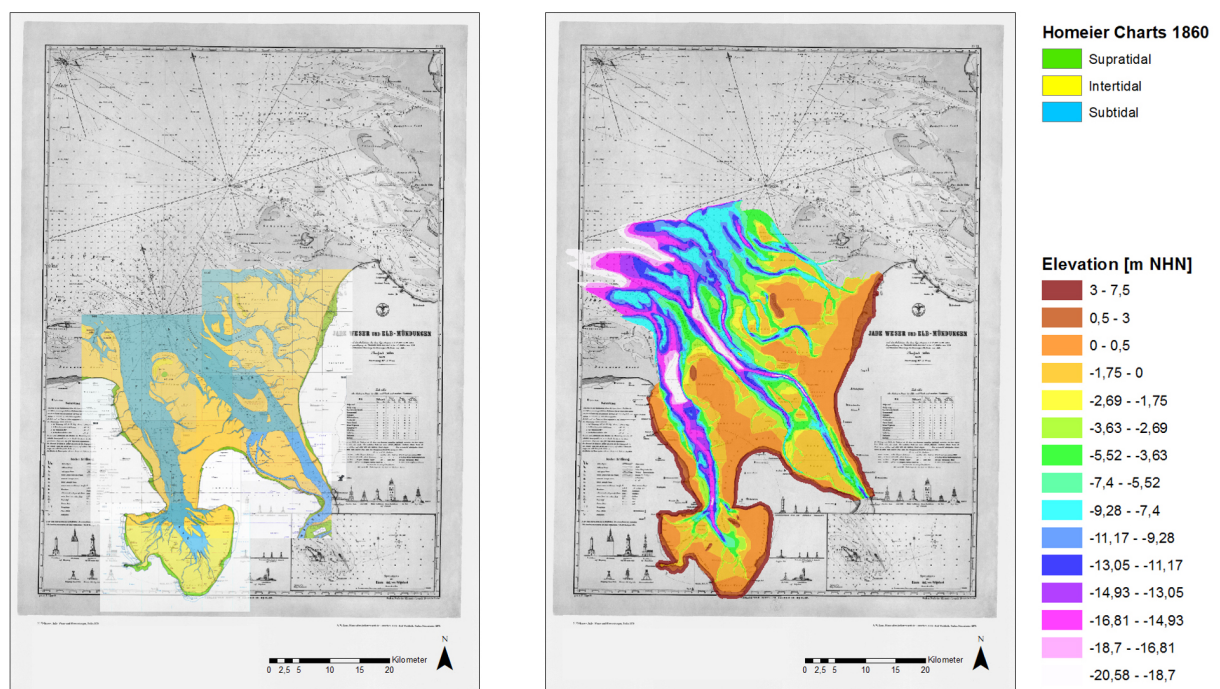


Figure 4: Homeier charts (Homeier et al. 2010) of the outer Weser and Jade estuary region for the state of 1860 showing supra-, inter- and subtidal areas (left panel) and Triangular Irregular Network (TIN) of the same region for the reconstructed state of 1870. The background shows a historical navigational chart of 1870 (Lang 1973) that was used to digitize the elevation data for the TIN.

2.2 Model Calibration

Due to the model setup and its completely new spatial domain covering a large area, the calibration process took a big share within the project. The ALE approach of the SCHISM model requires the calibration to iteratively optimize the model grid, since a specific range of very high CFL values has to be met. During the evaluation process of the study, necessary modifications of the grid resolution setup also had to be implemented continuously. The model was calibrated with and validated for different time periods from 2014 to 2017.

The overall results also strongly depend on the used turbulence closure scheme: The cross-scale domain shows depth variations between several thousand meters at the continental shelf and constantly wetting and drying cells next to tidal channels of 10 m depth in the Wadden Sea and estuaries.

Shallow water wave equation models, when turbulence is considered in a boussinesq-approximated way (e.g. two equation turbulence models) basically assume the complete water depth as the turbulent wall boundary layer.

Especially without meteorological or wave forcing at the surface, the specific configuration of the turbulence model may pose severe problems finding a realistic compromise between the open ocean and deeper North Sea areas and the Wadden Sea and estuaries. This is further complicated with vertical grid resolution issues.

The following parameters had to be considered in the calibration of the model:

- Horizontal grid and time stepping

The most important part was the design of the unstructured mesh in the horizontal plane, since the mathematical approach requires strict compliance with the appropriate CFL range. It has to accommodate optimal resolution of the investigation area in combination with a reasonable overall mesh size, time stepping and computational time. Several meshes for the same domain were set up and tested. Especially in the Wadden Sea and estuarine zone, the setups have developed intensely over time. Besides the implementation of quadrangular elements in the estuarine zone and stepwise refinement of the entire Wadden Sea from Den Helder to Esbjerg, a major step was to improve the grid design for Ems and Weser river, so that it can handle both historical and present states with flow-parallel quadrangular elements, even though positions and directions of the main channels differ greatly in some parts between the two conditions. Additionally, the model domain includes several areas between historical and present dyke lines. The current grid is optimized for a time stepping of 200 seconds.

- Vertical discretization

In the vertical plane, different solutions for discretization have been tested from 2D, pure z , hybrid sigma/ z -coordinates to localized sigma coordinates (Zhang et al. 2015). The current setup uses LSC² with a focus on the top 200 m, i. e. continental shelf.

- Bottom friction and turbulence closure scheme

The model was calibrated using different regional friction coefficients. The bottom friction is calibrated in alignment with present conditions and adopted for the historical states. This of course is a compromise and has the consequence, that results will not be satisfactory in all places and morphological states. But since friction is also one of the boundary conditions, this procedure ensures that we analyse differences induced only by bathymetrical changes and not from friction coefficient variations or

other boundary conditions. Bottom roughness is given as roughness length z_0 with a constant value of 2 mm.

- **Bathymetry**

As bathymetrical data is only accurate up to a certain level, it is valid and probably necessary to adjust it as a parameter in the calibration process in the range of its uncertainties (Verboom et al. 1991). Especially the historical bathymetries lack on accuracy, as stated before. Another problem evolves from the sparse density of the historical depth information. This leads to a great underestimation of the bed form resistance and existing dune structures, which cannot be compensated through roughness parameters. Therefore, these features are substituted by artificial surface irregularities that are added with a random distribution in the historical model parts.

The seaward open boundaries are driven with amplitudes and phases of 29 astronomical constituents, covering daily, fortnightly, monthly and seasonal inequalities of the tide. The nodal tide is represented with a constant node factor for each constituent. The amplitudes and phases of the constituents at the boundary nodes are interpolated from the FES Global Tides Model 2014. Constituent's Equilibrium arguments with reference to Greenwich and node factors are calculated within the SCHISM model suite on basis of Schureman (1940) for the starting and middle time of the simulation respectively.

The open boundaries at the tidal barriers of Ems, Weser and Elbe are supplied with discharge data. For some calibration runs we use daily discharge values measured at the gauges Versen (near Ems River tidal barrier), Intschede (Weser) and Neu-Darchau (Elbe). For the analysis though, we use approximate multiannual mean discharge values (see Table 4), as we only want to analyse the influence from bathymetrical changes under mean boundary conditions. Additional sources are set for Eider River and major tributaries along lower Ems and Weser.

Table 4: Constant discharge values at open boundaries and sources in the German Bight.

Rivers and tributaries	Position	Discharge <i>m³/s</i>	Source
Ems	At tidal barrier	80.0	Versen (rounded value), NLWKN 2018
Weser	At tidal barrier	300.0	Intschede (rounded value), NLWKN 2018
Elbe	At tidal barrier	700.0	Neu-Darchau (rounded value), HPA 2017
Leda	At tidal barrier	15.0	estimate
Hunte	At Weser inflow	15.0	Elsebach et al. 2007
Ochtum	At Weser inflow	7.5	Elsebach et al. 2007
Lesum	At Weser inflow	13.0	Elsebach et al. 2007
Geeste	At Weser inflow	5.0	Elsebach et al. 2007
Eider	Near Tönning	6.5	estimate

Atmospheric forcing is used within the calibration process to check the model performance under different meteorological conditions, even though the later analysis is carried out with astronomical tidal input only, because boundary conditions should remain the same between historical and present conditions and results should refer to mean tidal values and not be influenced by other boundary conditions. For the atmospheric calibration we use hourly forecast model data for air pressure, wind speed and wind direction from the ICON-Model of the German Meteorological Service (Deutscher Wetterdienst DWD).

The model results are compared to observation data of tide gauge stations along the British (10), Dutch (5) and German (55) coastline as well as from different offshore (5) stations. Figure 5 shows a selection of comparisons throughout the German Bight and inside the estuaries of Ems and Weser for the present morphological state as well as for gauge stations near the margins of the North Sea and offshore.

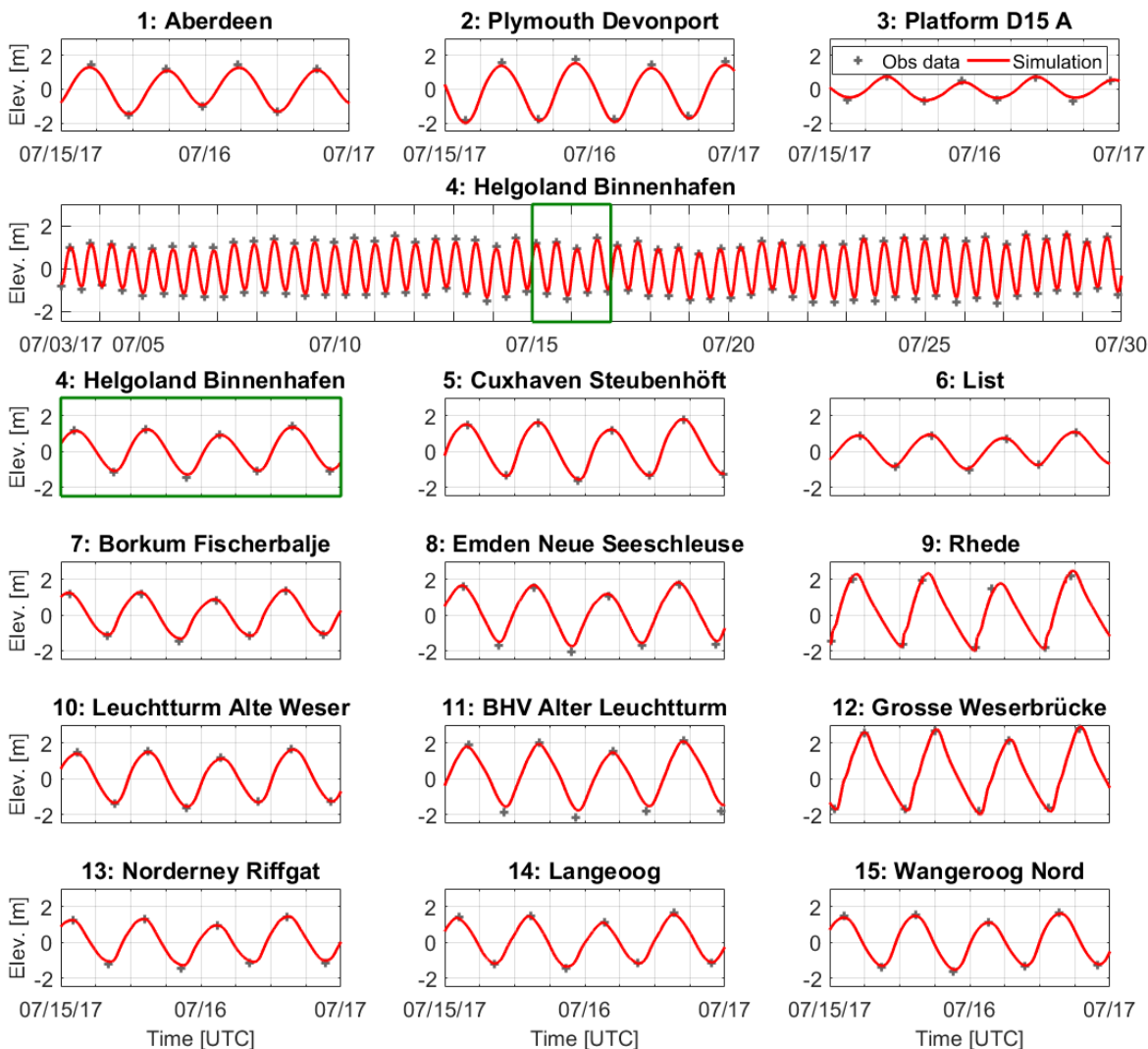


Figure 5: Comparison of Simulation (red) to Observation (gray) data at selected gauge stations. Positions are indicated in Figure 6. Observation data provided by WSV, British Oceanographic Data Centre and Rijkswaterstaat.

Figure 6 displays the Root mean square error (RMSE) for both High and Low water values at selected gauge stations in the German Bight. The upper panel shows the combined RMSE. Along the coastline the RMSE is satisfactory with values below 10 cm. Inside the estuaries, especially for low water conditions, there is a misfit between observation and simulation at some stations. This applies near the tidal barrier of the Ems River and around Bremerhaven and Nordenham in the Weser River. It is assumed that this is due to the rheological influence of the fluid mud and the dynamics of the estuarine circulation, since turbidity and density induced turbulence damping is not included in the calculations. As the pure hydrodynamic model cannot reproduce these effects, the calibration concentrates

on a best overall fit in space (different tidal gauge stations) and time (different morphological states).

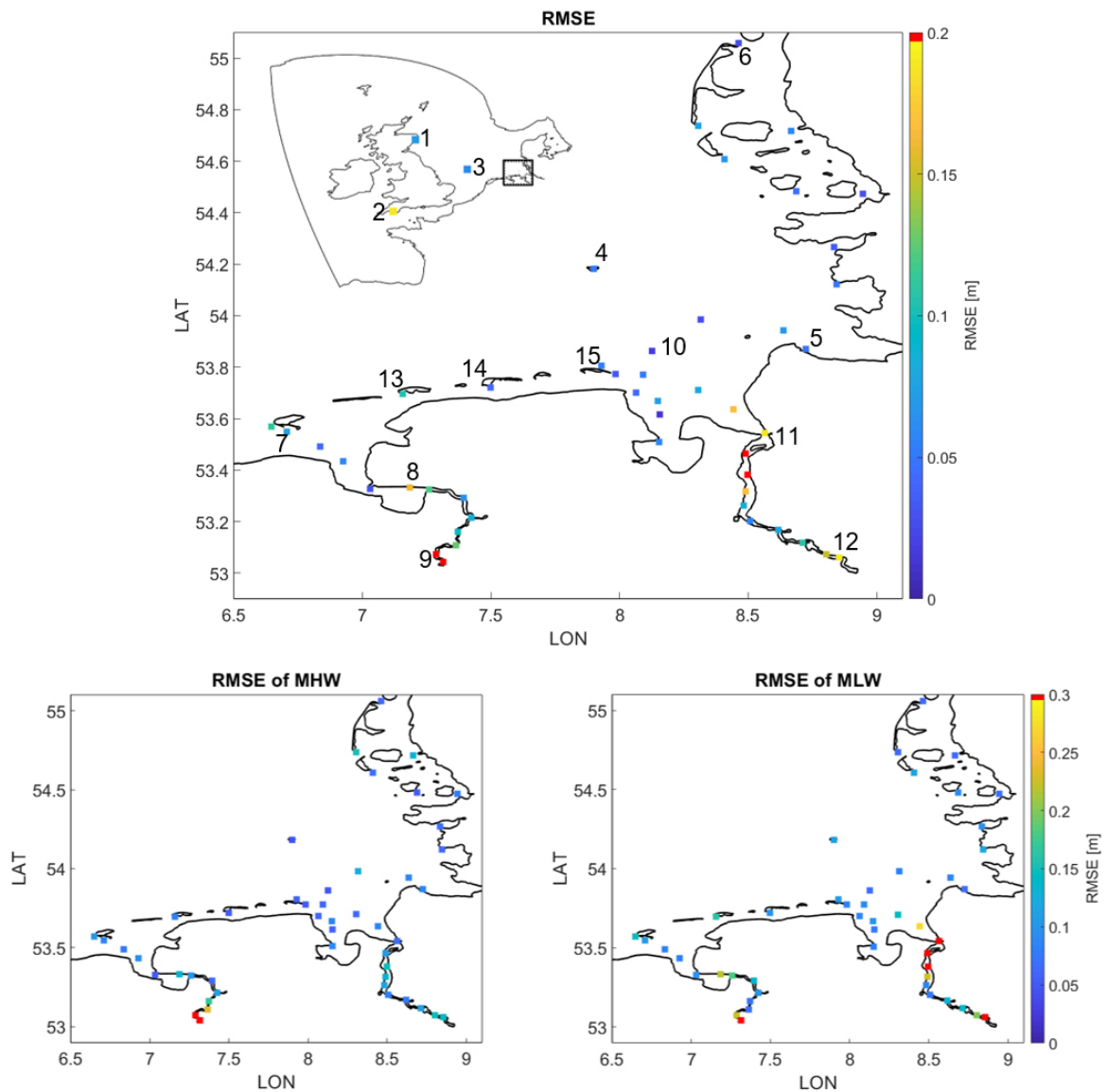


Figure 6: Root Mean Square Errors (RMSE) for tide gauges in the German Bight (present morphological state). Lower panels display RMSE for High and Low water values, upper panel the combined RMSE. Numbers in upper panel indicate position of plots in Figure 5.

Figure 7 shows results in comparison to observation data for a model run with storm surge conditions during January 2017 at the Dutch gauge station Huibertgat, which plays an important role in the calibration process, as its position close to the Dutch-German border is in tidal luv of the investigation area along the German Coastline. The results show that the model is able to perform both in calm weather and storm surge conditions. Atmospheric forcing is driven with forecast model data from the ICON-Model (DWD). As this is no observation data, disagreements between modelled and observed water level can also be due to under- or overestimated atmospheric parameters in the forecast model. The upper panel shows water level elevation, lower three panels show air pressure, wind speed and wind direction respectively.

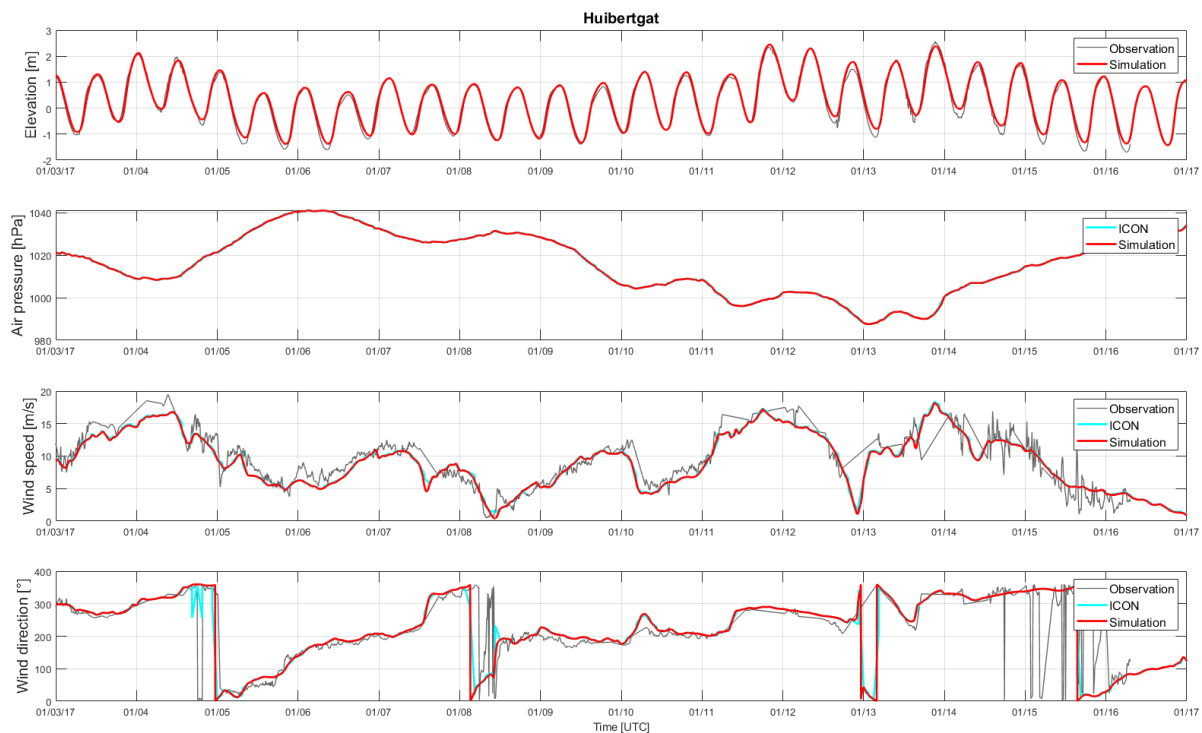


Figure 7: Comparison of simulation (red) to observation (grey) and forecast model (light blue) data at gauge station Huibertgat during a time period with storm surge conditions in the German Bight (January 2017). Huibertgat is offshore the most eastern Dutch barrier islands Schiermonnikoog and Rottumerplaat. Observation data provided by Rijkswaterstaat.

Since for most gauge stations available historical single water level values are rare, we use multiannual mean values to compare the model results from historical bathymetries. In Figure 8 there are comparison plots for different gauge stations along the Weser estuary. The plots are ordered in upstream direction. The results were produced without meteorological forcing and with an arbitrary astronomical constellation, as we do not compare to a specified period but to multiannual mean values. In order to meet the observations better, mean sea level for calibration of the model was lowered by 25 cm. The discharge time series is artificial. It consists of discharges between approximately half to double of the mean discharge ($300 \text{ m}^3/\text{s}$) at the tidal barrier, which roughly meets the late 19th century as well as today situation (Elsebach et al. 2007). The thin grey tide curve in the background displays the tide under present conditions. It does not represent observation data, but also modelled data from a simulation with the present bathymetry and exactly the same boundary conditions. The difference between the red and the thin grey lines demonstrates the drastic change in tidal regime between the two morphological states, as already displayed in Figure 2. The horizontal dark grey dashed lines represent the five yearly mean tidal values at the corresponding gauge station for the year indicated in the legends. The shaded range illustrates minimum and maximum values of the corresponding five-year period. Further upstream, these ranges grow bigger, as influence from discharge grows with decreasing influence from the tides. The modelled results show the same behaviour. The tidal range at Große Weserbrücke is significantly smaller and the water level oscillates along with variations in discharge values around the historical mean values. In contrast, under present conditions (thin grey lines), discharge-differences are hardly notable close to the tidal barrier.

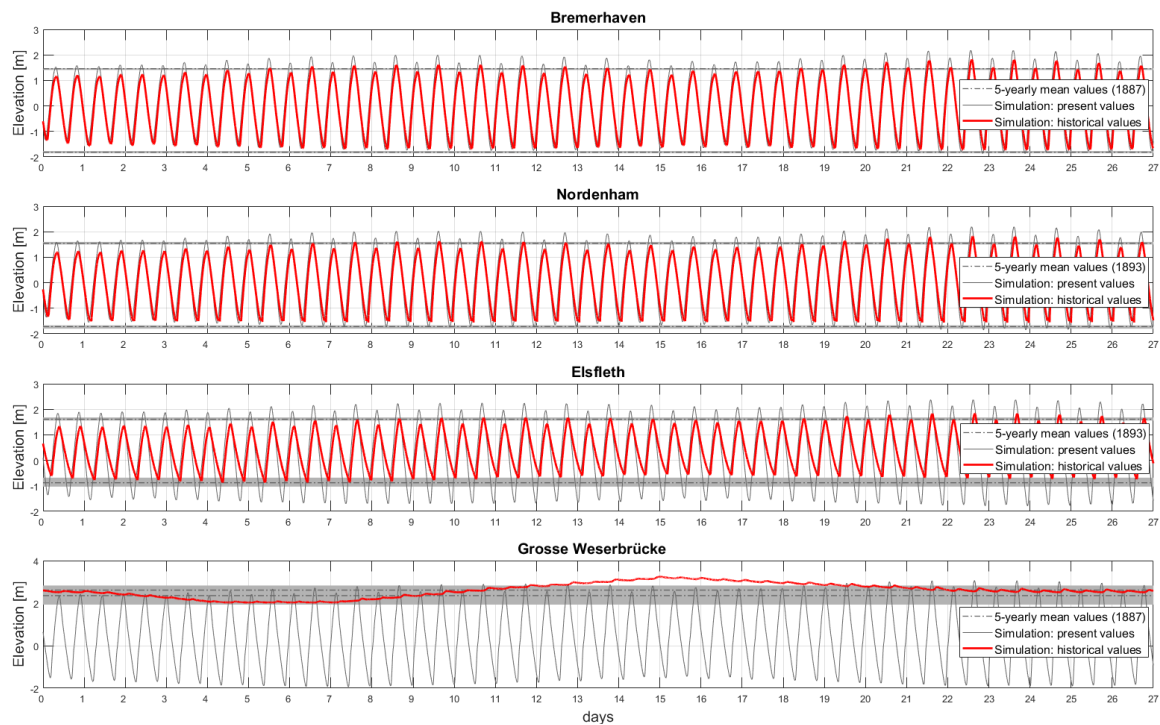


Figure 8: Comparison of simulated historical (red) and present (thin grey) tide to historical multi-annual mean values (dashed grey lines and shaded areas) along the Weser estuary in upstream direction. Positions can be seen in Figure 9.

Differences of the tidal regime not only at selected gauge stations but along a transect of the Weser river with a discretization of 1 km is demonstrated in Figure 9. The upper and middle left panels show synthesized mean tidal curves (for explanation see Section 3) for every km of the tidal Weser river from km 0 to km 126 for historical (upper) and present (middle panel) morphological conditions. The positions are indicated in the lower left panel with the corresponding colour. The grey dots show the historical pathway of the main channel in the outer Weser before the Franzius corrections. Tidal curves are plotted over time beginning with high water at km 0. The dashed lines represent positions approximately at gauge stations (see legend. Not all gauge stations were already in operation in 1887 – they serve as orientation in the plots).

The plots again reveal the change of the tidal regime. The tidal range increases especially further upstream. The tidal phases shift along the transect, as under historical conditions, the tidal wave took longer to reach from outer Weser to Bremen. Finally, the decrease of the water level gradient can be derived from the figures. Present tidal curves are closely grouped. The right panels show different tidal wave lines and envelope curves of high and low waters along the transect for historical (upper three panels) and present time (middle three panels) and in comparison of both states (lower right panel). The small crosses show observation data.

Along the historical transect, simulated low water conditions remain significantly above the observed mean values, especially upstream of Vegesack. One reason for this is the sparse bathymetrical information and chosen assumptions (no calibration over friction, same roughness parameters as in present run). The representation of the historical tributaries Ochtum and Lesum might also be problematic here. They are represented in the model with substitute systems, but their share of the tidal volumes that the rivers would withdraw from the Weser in historical times can only be roughly estimated. Franzius (1888)

stated that before the corrections, upstream of Ochtum and Lesum only half of the tidal volume would progress to Bremen. This might explain why the model is hardly able to rise low water crests according to observation data. This means that the numerical model still underestimates the tidal regime changes and that results are a rather conservative estimate.

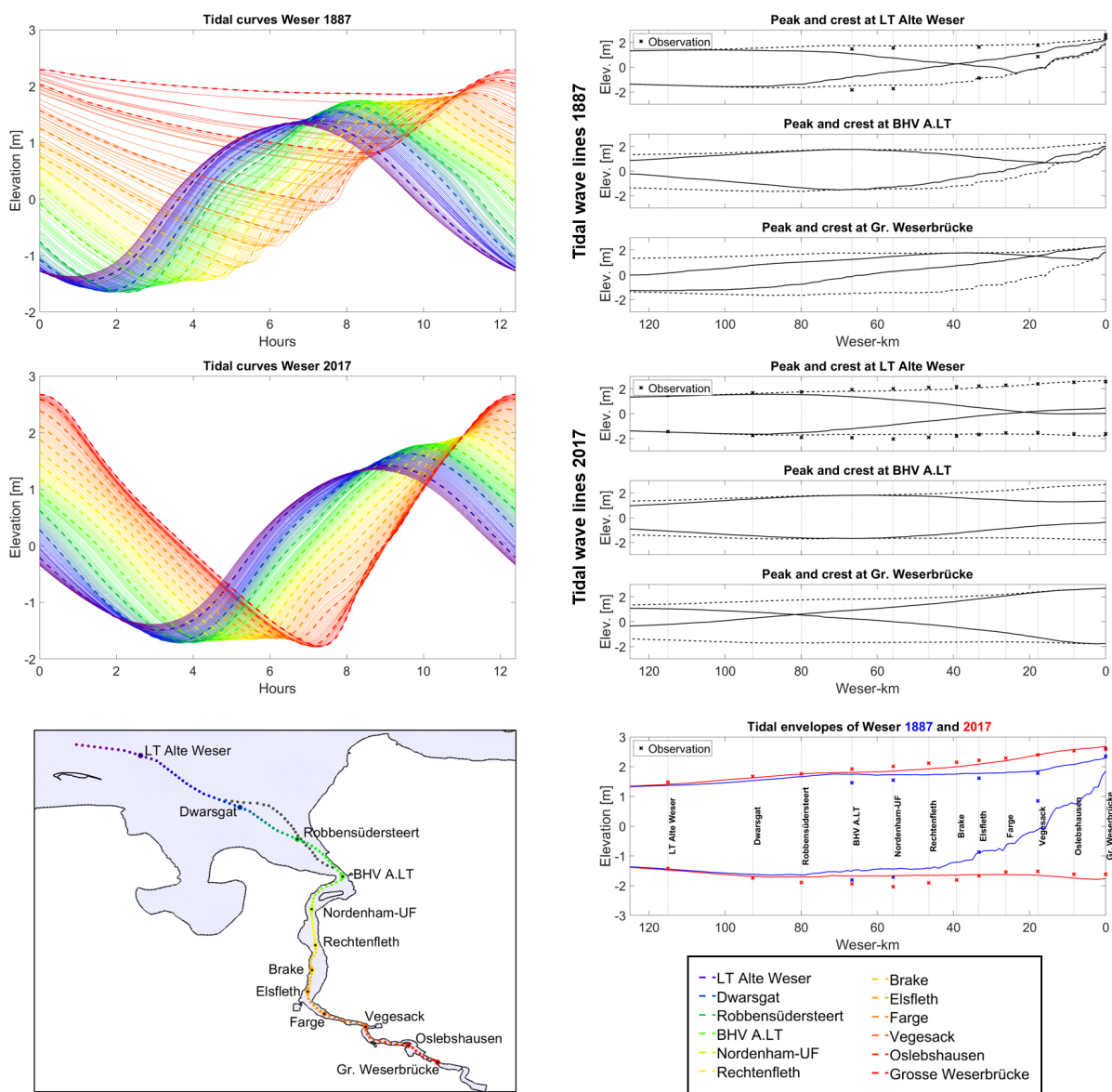


Figure 9: Left panels show modelled tidal curves at different positions at longitudinal sections of the tidal Weser River for both the historical (1887, top panel) and present (2017, middle panel) morphological state. Dashed lines indicate position near tidal gauge stations (bottom right legend). Bottom left panel indicates the corresponding position of the tidal curves and gauge stations. Right panels show tidal wave lines along the same longitudinal sections for the historical (top three panels) and present (middle three panels) states for different positions of tidal peaks and crests. The dashed lines show the envelope curves for all possible tidal wave lines. The bottom right panel shows a comparison of the modelled envelope curves of historic (blue) and present (red) state. The crosses indicate observed tidal high and low water values from tide gauge records.

In the case of baroclinical calibration, open boundaries are set to a constant value of 35.0 PSU at the seaward and 0.3 PSU at riverine open boundaries. The domain is initiated with a hotstart file, that was previously ramped-up for 30 days with initial PSU between 32

and 34 on the shelf and <32 to 0.5 in the estuaries. Analysis though are carried out barotropically without solving for transport equations. Salinity plays an important role for sea level heights, especially in the estuarine zone, where the density gradient influences the elevation in the range of several centimetres. But when comparing only the differences between historical and present tidal characteristics rather than looking at absolute values, the differences remain nearly the same for both barotropic and baroclinical simulations in the coastal zone, as the influence from density evens out here (see Figure 10, bottom left panel in comparison to top right panel). Because the advantages due to baroclinical simulation regarding the outcome in the coastal zone is rather small compared to the strongly increased computational effort, simulations are carried out barotropically without solving for transport equations. Another reason contradicting the baroclinical approach is the difficulty to calibrate the historical model for salinity, as there is no sufficient data.

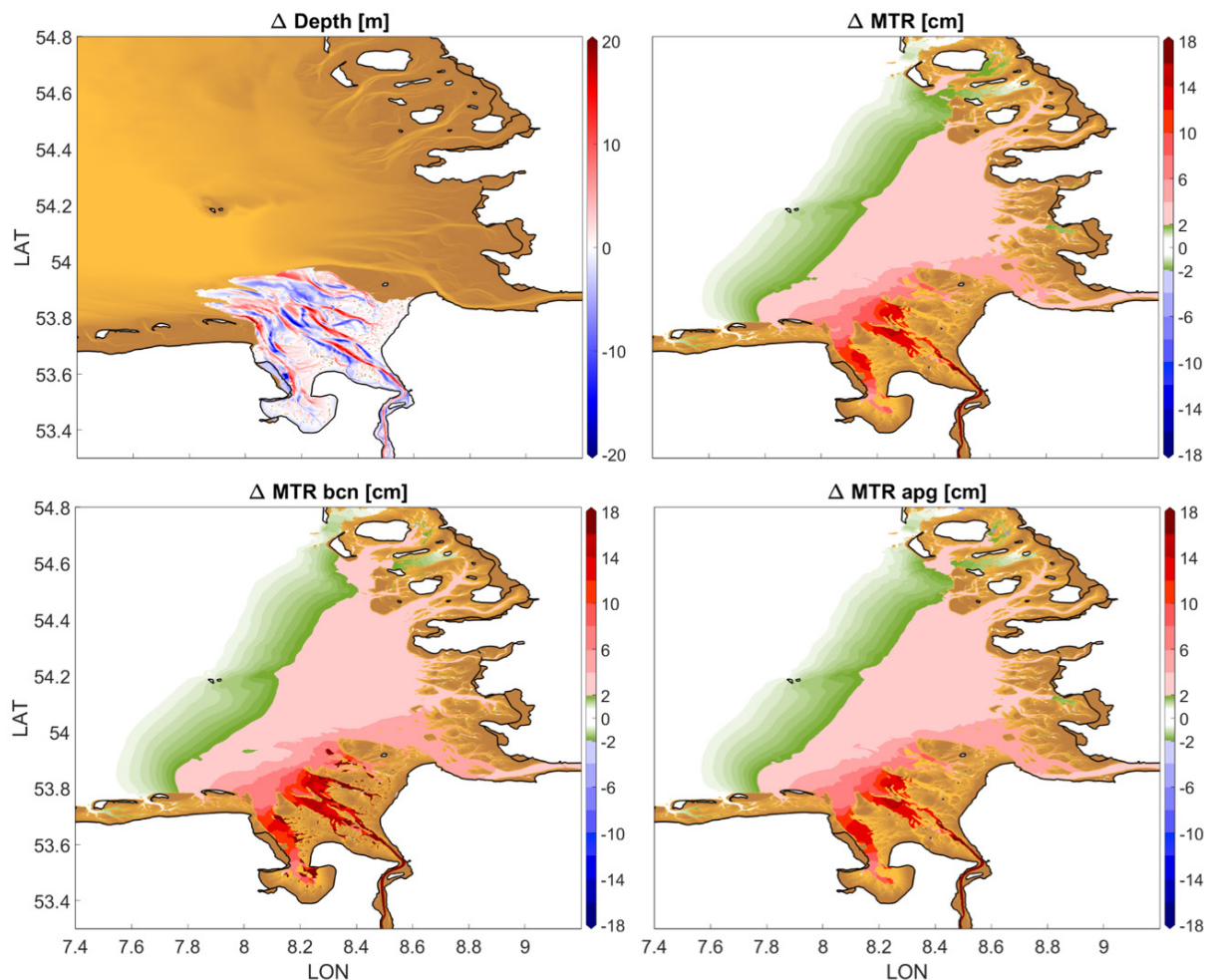


Figure 10: Model differences of bathymetry on top overall bathymetry (top left) and difference of mean tidal range values for the control run minus the setup of the historical lower and outer Weser and Jade estuaries in barotropic mode (top right), baroclinic mode (bottom left) and evaluated for only half of the simulation period (here, the slightly higher apogean spring-neap-cycle, bottom right). The top panels are adopted from Figure 13 in Section 3.

The differences between perigean and apogean tides also even out when comparing water level differences. The first estimations intended that it seemed important for the results to include at least two spring-neap cycles. But analysis showed that despite differences of up

to several centimetres in absolute values, the effect cancels out when comparing the differences between historical and present morphological states (see Figure 10, bottom right panel in comparison to top right panel).

3 Results

The computation of the synthesized mean tidal curves is similar to the evaluation of a tidal record with a so-called “Auswerteharfe” (Hensen 1954). The simulations are carried out over a period of 32 days without atmospheric forcing. The first two days are omitted as ramp-up period. The remaining 30 days assure that the simulation contains results of at least two spring-neap cycles with diurnal, fortnightly and monthly inequalities of the tide (compare left panels in Figure 11). For every computational node of the domain, peak values, i. e. tidal high waters, are detected. The first and last value are again omitted, leaving – in general – 56 tidal high waters. All values of the 55 tidal cycles between two consecutive tidal highs are interpolated on a grid of 12.4 hours with a discretization of six minutes. The average of all of these interpolations is the synthesized mean tidal curve of the corresponding computational node (compare right panels in Figure 11). The procedure can be repeated with other values like u- and v-velocities. This allows to derive different hydrodynamic mean values for the whole domain like mean tidal high and low water values, flood and ebb phase durations, maximum flood and ebb velocities, residual currents and others.

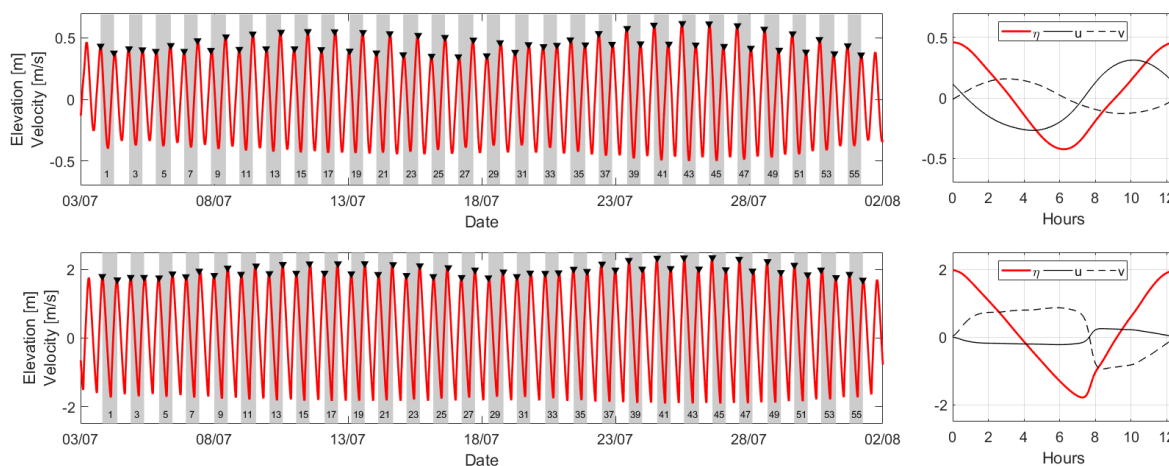


Figure 11: Left panels: Simulated tidal record (red) over 30 days for an arbitrary point in the North Sea (top) and near Weener, Ems (bottom). Black markers indicate tidal peaks, small integers indicate tide numbers. Right panels: Synthesized mean tidal curves for elevation (red), u- (black) and v-velocity (dashed) derived from the 55 tidal cycles in the left panel.

Before showing results for the Ems and Weser estuary, the evaluation process shall be demonstrated in a first small scale example. The Hindenburgdamm, built in the 1920’s, connects the island of Sylt with the mainland. Figure 12 shows how this dam influences the tidal characteristics in the area around Sylt. The model bathymetry has only been changed around the dam in the slightly blue shaded area in the upper left panel. The remaining bathymetry and all boundary conditions are equal to those of the control run. Consequently, the figure does not show how the real tidal characteristics have changed since the construction of the dam, but rather illustrate the sensitivity for the present morphological condition with and without the Hindenburgdamm.

The anti-clockwise rotating tidal wave propagates in northward direction at Sylt and thus is dammed behind the island. Consequently, the dam increases the tidal range (top right panel) and tidal high waters (bottom left panel) in the southern tidal basin and decreases them in the northern tidal basin. As the dam is positioned on the watershed divide between the two basins, there is no effect on low water conditions (bottom right panel).

Due to the strongly implicit character of the model, which enables the cross-scale approach in the first place, small numerical disturbances, i. e. caused from the wetting and drying algorithm, can propagate far off their place of origin, as Courant numbers are large. These disturbances can be observed in remote places of the domain, which cannot be related to local morphological changes. No explicit disturbances of this kind are shown in the results of the following figures, but since the wetting/drying-induced noise can be found up to two centimetres in range and cannot unambiguously be differentiated from the physical effect, all differences within this range, regardless of their vicinity to the morphological changes, are shaded differently in green colour.

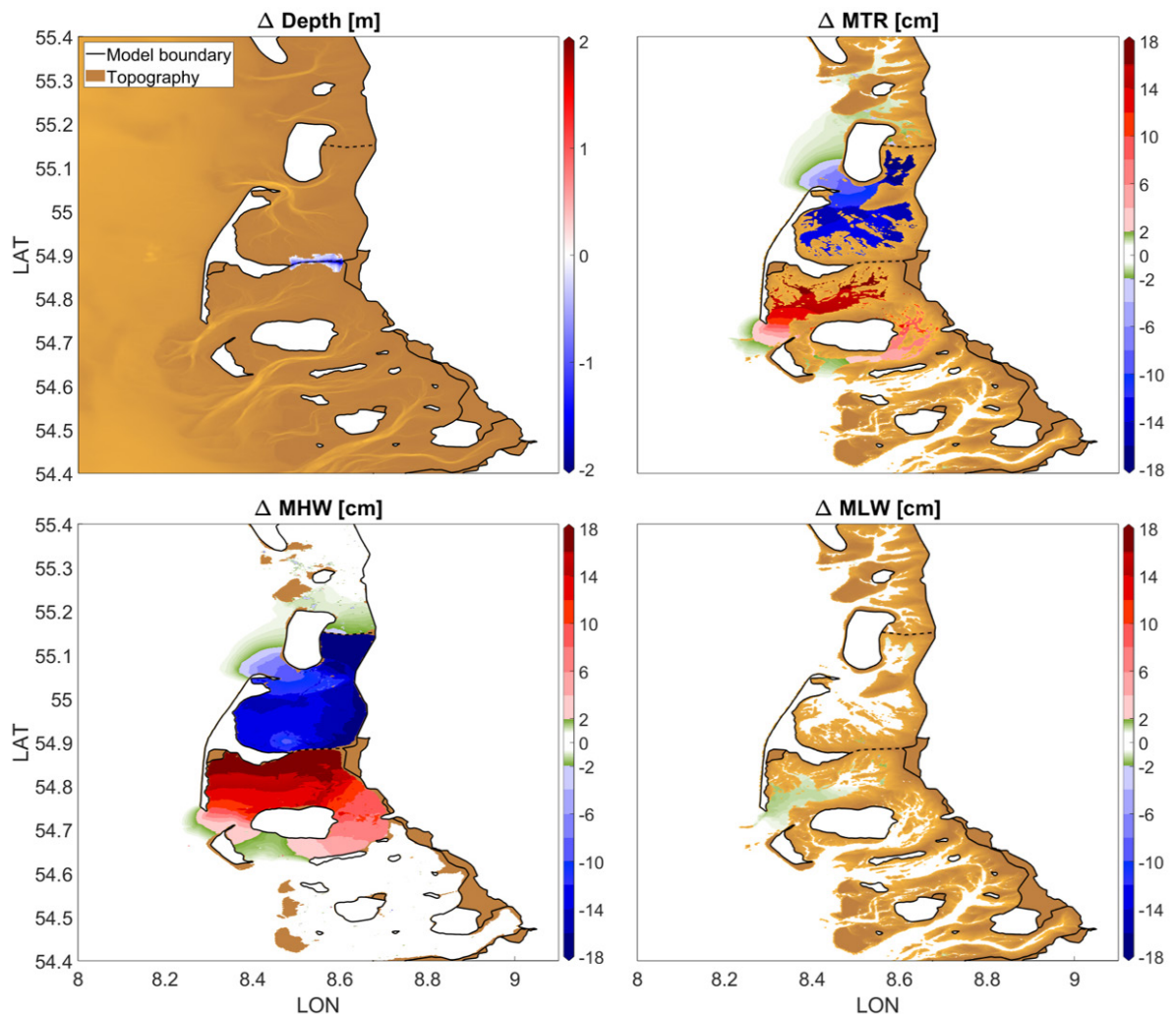


Figure 12: Model differences of bathymetry on top overall bathymetry (top left), mean tidal range (top right), mean tidal high (bottom left) and low (bottom right) water conditions for the control run minus the setup without the Hindenburgdam.

For the Weser estuary we compare two different historical setups in Figure 13. In the first setup, the bathymetry has only been changed in the lower Weser estuary, i. e. from Bremerhaven up to Bremen. In the second setup, the historical states of the outer Weser and Jade have also been considered in the simulation.

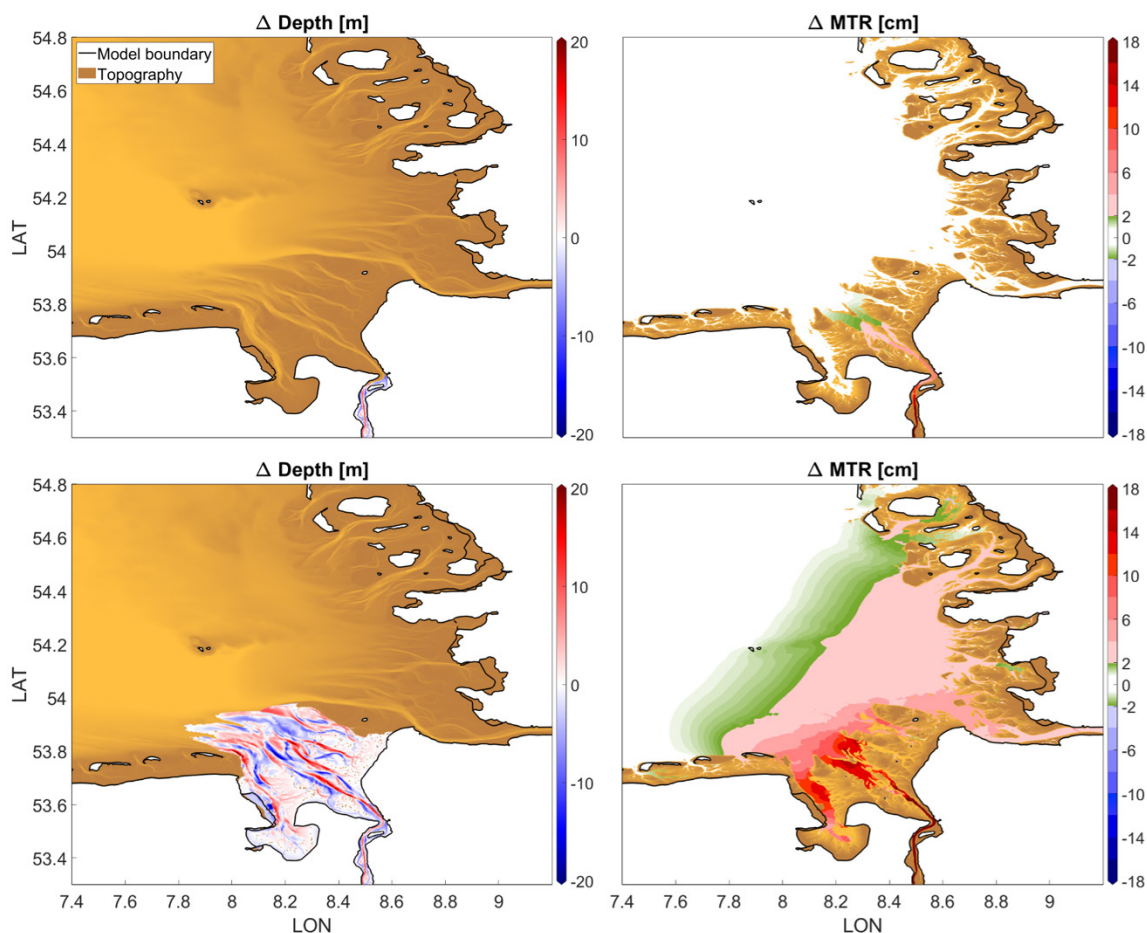


Figure 13: Model differences of bathymetry on top overall bathymetry (left) and mean tidal range values (right) for the control run minus the setup of the historical lower Weser estuary (top) and minus the setup of the historical lower and outer Weser and Jade estuaries (bottom) respectively.

The right panels show the modelled differences of the mean tidal range between the present and the two corresponding historical states and how far the changes reach outside of the region with changed bathymetry. The reader should be aware that River Elbe is included with its present topography for both runs.

Whereas for the first (upper) setup changes are found up to Dwarsgat (position indicated in Figure 9), changes of the second (bottom) setup influence the tide far beyond the margins of the changed bathymetry up to the coast of Schleswig-Holstein to small extends of a few centimetres. The influence of the changed topography is notably stronger in the anti-clockwise net-direction of the tidal wave propagation.

Also the evaluation of the Ems estuary shows an anti-clockwise shift of the differences (see Figure 14, right panel), even though changes above two centimetres seem to remain mainly within the area, where model bathymetry has been changed – in this case lower and outer Ems estuary.

In both cases, the MTR-rise is the result of decreasing MLW and increasing MHW.

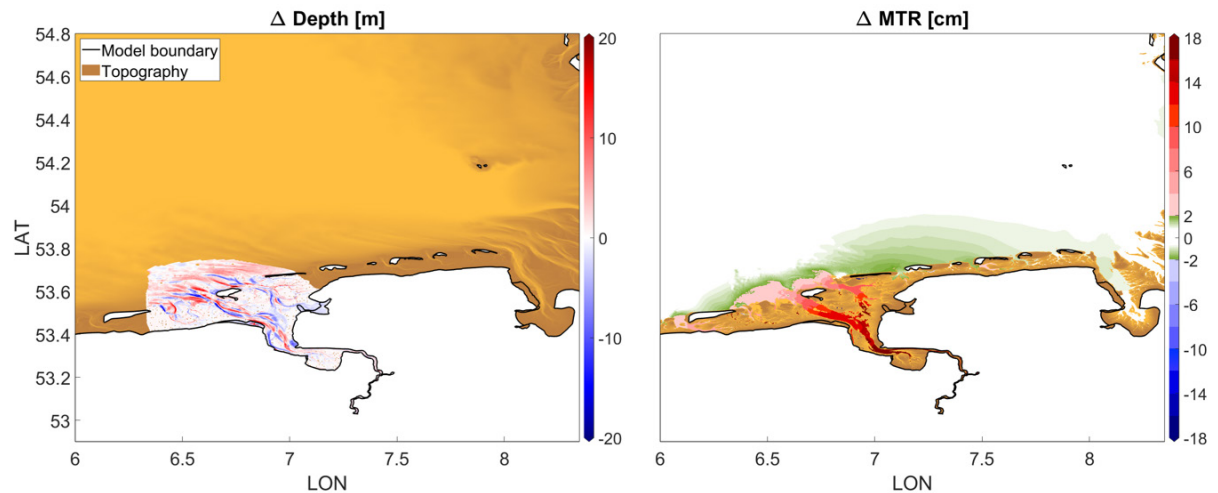


Figure 14: Model differences of bathymetry on top overall bathymetry (left) and mean tidal range values (right) for the control run minus the setup of the historical lower and outer Ems estuary.

Part of the research project was to analyse effects that are caused from land subsidence due to gas extraction from the gas field of Groningen, as subsidence, in this case manmade, influences the relative sea level directly (Fokker et al. 2018). The Groningen gas field is located close to the Ems estuary and is supposed to be the largest onshore gas field in Western Europe (NAM B.V. 2016). Figure 15 shows measured and modelled subsidence values of the Ems-Dollard region from 1972 to 2013 that were collected within the continuous monitoring process of the gas field (NAM B.V. 2015). It can be seen that the subsidence reaches into the Ems estuary, even though only with small absolute values ranging from approximately two to 22 cm, mostly in the area of Paapsand, a tidal flat west of the navigational channel of the Ems. Subsidence from neighbouring German gas fields is not included, as there is no monitoring program collecting data. Besides that, output volumes from the German gas fields are significantly smaller than those from the Groningen gas field (LBEG 2018).

The subsidence values were transferred into a TIN and subtracted from the depth of the model grid in order to simulate differences to the control run.

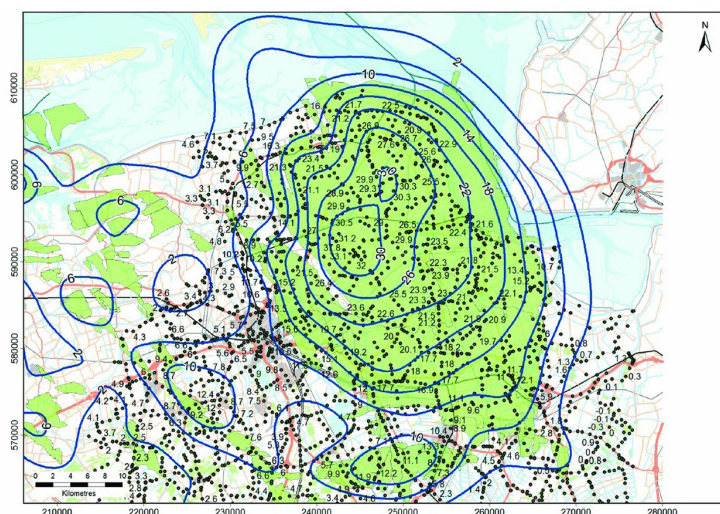


Figure 15: Measured and modelled subsidence values in the Ems-Dollard region for the period 1972–2013. Green areas show gas fields, black dots measured subsidence at benchmarks and blue lines contour-lines of modelled subsidence (NAM B.V. 2016).

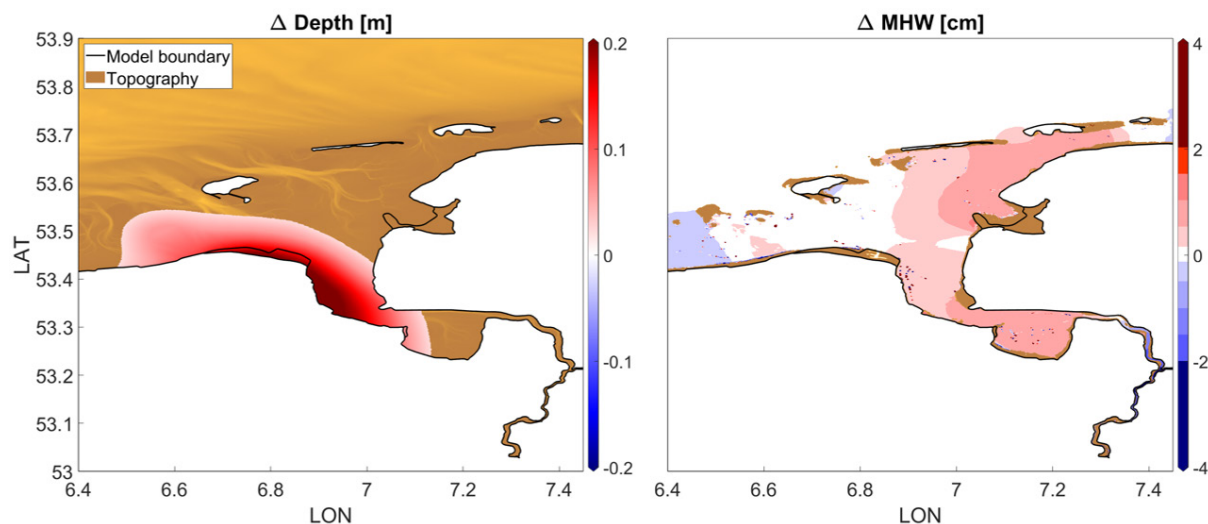


Figure 16: Model differences of bathymetry (red) on top overall bathymetry (left) and mean tidal range values (right) for the control run minus the setup of subsidence values from gas extraction in the gas field of Groningen. Mind the different scale in comparison to the other figures.

The results show that the influence from gas extraction in the Groningen gas field on single tidal characteristics in the Ems estuary remains small in comparison to the impact it has on the vertical land movement. The major part of the differences is below one cm (see Figure 16, right panel). The figure only shows results for mean tidal high-water conditions, because the greatest subsidence occurs in areas that fall dry during low water.

4 Summary

The setup and application of a cross-scale numerical model to analyse the influence of morphodynamical and man-made changes in the estuarine zones of the Lower Saxonian coast on tidal dynamics in adjacent regions was introduced.

Reproductions of morphological states of past and present times have been used to evaluate differences of the tidal regimes and visualize the reach of these changes into unmodified regions of the model. The results show that local changes of the bathymetry can influence the tidal regime even far offside the place of action, especially in the leeward direction of the tidal wave propagation.

The results give an estimate of the contribution of historically large estuarine river construction measures to tidal regime changes. The lack of historical data requires several assumptions in the model and boundary conditions to be made.

The results give a good impression of the man-made contribution to observed long-term trends in mean high and low water measurements, which is a new and relevant contribution to the interpretation of those data in the context of mean sea level rise and climate change driven effects.

5 Acknowledgements

We would like to thank our project partners from the Research Institute for Water and Environment at the University of Siegen and the Institute of Coastal Research at the Helmholtz-Zentrum Geesthacht for the collaboration and their contributions. ALADYN-C

is funded by the German Federal Ministry of Education and Research (BMBF) under the reference 03F0756C.

6 References

Ateljevich, E.; Zhang, Y.; Nam, Kijin: Hydraulic Structures in SELFE. California Department of Water Resources, 2014.

BUND: Fahrwasservertiefungen der Unter- und Außenweser. Bund für Umwelt und Naturschutz Deutschland, Landesverband Bremen. Retrieved on Nov. 2018: http://archiv.bund-bremen.net/fileadmin/bundgruppen/bcmlsvbremen/naturschutz/weservertiefung/Weservertiefungen_UEbersichtstabelle.pdf.

DWD: ICON (Icosahedral Nonhydrostatic) Model, Deutscher Wetterdienst, Offenbach. Retrieved on Jun. 2018: https://www.dwd.de/SharedDocs/downloads/DE/modelldokumentationen/nwv/icon/icon_dbbeschr_aktuell.pdf?view=na&Publication&nn=495490

Elsebach, J.; Kaiser, R.; Niemeyer, H. D.: Identifikation von erheblich veränderten Gewässerbereichen in der Tideweser. Untersuchungsbericht der NLWKN Forschungsstelle Küste 05/2007, Norderney, 2007 (unpublished).

EasyGSH-DB: Erstellung anwendungsorientierter synoptischer Referenzdaten zur Geomorphologie, Sedimentologie und Hydrodynamik in der Deutschen Bucht (EasyGSH-DB). Retrieved on Apr. 2018: <https://www.mdi-de.baw.de/easygsh>

EMODnet: European Marine Observation Data Network. Retrieved on Jan. 2017: <http://www.emodnet.eu/bathymetry>

FES: Finite Element Solution Global Tide Model 2014. FES2014 was produced by Noveltis, Legos and CLS Space Oceanography Division and distributed by Aviso, with support from Cnes. Retrieved on Okt. 2017: <http://www.aviso.altimetry.fr/>

Fokker, P. A.; van Leijen, F. J.; Orlic, B.; van der Marel, H.; Hanssen, R. F.: Subsidence in the Dutch Wadden Sea. In: Netherlands Journal of Geosciences, 97–3, 129–181, <https://doi.org/10.1017/njg.2018.9>, 2018.

Franzius, L.: Die Korrektur der Unterweser. Bremische Deputation für die Unterweser-korrektur, Bremen, 1888.

Haigh, I. D., Pickering, M. D., Green, J. A. M., Arbic, B. K., Arns, A., Dangendorf, S., et al.: The tides they are a-changin': A comprehensive review of past and future nonastromonomical changes in tides, their driving mechanisms and future implications. In: Reviews of Geophysics, 57, <https://doi.org/10.1029/2018RG000636>, 2020.

Herrling, G.; Niemeyer, H. D.: Reconstruction of the historical tidal regime of the Ems-Dollard estuary prior to significant human changes by applying mathematical modeling. HARBASINS Report, <https://www.nlwkn.niedersachsen.de/download/70706>, 2007a.

Herrling, G.; Niemeyer, H. D.: Long-term Spatial Development of Habitats in the Ems-Dollard Estuary. HARBASINS Report, <https://www.nlwkn.niedersachsen.de/download/7070>, 2007b.

Herrling, G.; Niemeyer, H. D.: Comparison of the hydrodynamic regime of 1937 and 2005 in the Ems-Dollard estuary by applying mathematical modeling. HARBASINS Report, <https://www.nlwkn.niedersachsen.de/download/70703>, 2008.

Herrling, G.; Elsebach, J.; Ritzmann, A.: Evaluation of Changes in the Tidal Regime of the Ems-Dollard and Lower Weser Estuaries by Mathematical Modelling. In: *Die Küste*, 81, 2014.

Hensen, W.: Modellversuche für die untere Ems. Mitteilungen der Hannoverschen Versuchsanstalt für Grundbau und Wasserbau. Franzius-Institut der Technischen Hochschule Hannover. Hannover, 1954.

Homeier, H.; Stephan H.-J.; Niemeyer, H. D.: Historisches Kartenwerk Niedersächsische Küste der Forschungsstelle Küste. Berichte der Forschungsstelle Küste. Band 43/2010, Norderney, 2010.

Hubert, K.; Wurpts, A.; Berkenbrink, C.: Modelling the Impact of Estuarine and Coastal Morphological Changes on Tidal Dynamics in the German Bight. In: E-proceedings of the 38th IAHR World Congress September 1–6, 2019, Panama City, <https://doi.org/10.3850/38WC092019-0799>, 2019.

HPA: Deutsches Gewässerkundliches Jahrbuch Elbegebiet Teil III 2014. Hamburg Port Authority, Hamburg, 2017.

Lang, A. W.: Historisches Seekartenwerk der Deutschen Bucht. No 78 Grapow, Jade-, Weser- und Elbmündungen, Berlin 1870. Karl Wachtholtz Verlag, Neumünster 1973.

LBEG: Erdöl und Erdgas in der Bundesrepublik Deutschland 2017. Landesamt für Bergbau, Energie und Geologie. Hannover, 2018.

NAM B.V.: Bodemdaling door aardgaswinning. NAM-velden in Groningen, Friesland en het noorden van Drenthe. Status rapport 2015 en Prognose tot het jaar 2080. Nederlandse Aardolie Maatschappij B.V., Assen, 2015.

NAM B.V.: Winningsplan Groningen Gasveld 2016, 2016. https://www.nam.nl/algemeen/mediatheek-en-downloads/winningsplan-2016/_jcr_content/par/textimage_996696702.stream/1461000524569/1d3f1162f0dbba3f15b8bbc2c7087224fb413ce1/winningsplan-groningen-2016.pdf, Request: Okt. 2017.

Niemeyer, H. D.; Kaiser, R.: Mittlere Tidewasserstände. In: *Umweltatlas Wattenmeer*. Band 2: Wattenmeer zwischen Elb- und Emsmündung. Nationalparkverwaltung Niedersächsisches Wattenmeer, Umweltbundesamt. Wilhelmshaven, Berlin, 1999.

Niemeyer, H. D.: Prüfung der Sturmflutsicherheit in Brake zwischen Weserlust und Haus Linne. NLÖ Forschungsstelle Küste, Norderney, 2000 (unpublished).

NLWKN: Deutsches Gewässerkundliches Jahrbuch Weser- und Emsgebiet 2015. Niedersächsischer Landesbetrieb für Wasserwirtschaft, Küsten- und Naturschutz, Norden, 2018.

Portal Tideweser: Weseranpassung. Wasserstraßen- und Schifffahrtsverwaltung. Retrieved on Jul. 2019: <https://www.kuestendaten.de/Tideweser/DE/Projekte/Weseranpassung/Weseranpassung-node.html>

Schureman, Paul: Manual of Harmonic Analysis and Prediction of Tides. Special Publications No. 98. U.S. Department of Commerce, 1940.

See- und Ozeanhandbücher: Nr. 2006: Nordsee, östlicher Teil. Von Hanstholm bis Terschelling. Deutsches Hydrographisches Institut, Hamburg, 1958.

Verboom, G. K.; de Ronde, J. G.; van Dijk, R. P.: A fine grid tidal flow and storm surge model of the North Sea. In: *Continental Shelf Res.*, 12, 1991.

Zhang, Y.; Ateljevich, E.; Yu, H-C.; Wu, C-H.; Yu, J. C. S.: A new vertical coordinate system for a 3D unstructured-grid model. In: *Ocean Modelling*, 85, 16–31, 2015.

Zhang, Y.; Ye, F.; Stanev, E. V.; Grashorn, S.: Seamless cross-scale modeling with SCHISM. In: *Ocean Modelling*, 102, 64–81, 2016.